Nitric Oxide Inhibition of Free Radical-Mediated Cholesterol Peroxidation in Liposomal Membranes†

Witold Korytowski,‡,§ Mariusz Zareba,§ and Albert W. Girotti*,§

Department of Biochemistry, Medical College of Wisconsin, Milwaukee, Wisconsin 53226, and Institute of Molecular Biology, Jagiellonian University, Krakow, Poland

Received February 18, 2000; Revised Manuscript Received March 29, 2000

ABSTRACT: The ability of nitric oxide (•NO) to inhibit propagative lipid peroxidation was investigated using unilamellar liposomes (LUVs) constituted with egg phosphatidylcholine (PC) or 1-palmitoyl-2-oleoylphosphatidylcholine (POPC), [^{14}C]cholesterol (Ch), and a nonregenerable singlet oxygen-derived primer, 5α-hydroperoxycholesterol (5α-OOH). Exposing LUVs to ascorbate and a lipophilic iron chelate at 37 °C resulted in an exponential decay of 5α-OOH and accumulation of free radical-derived 7α- and 7β-hydroperoxycholesterol (7αβ-OOH), as detected by high-performance liquid chromatography with electrochemical detection. Thiobarbituric acid-reactive species (TBARS) were generated concurrently in egg PC-containing LUVs. Including the •NO donor spermine NONOate (SPNO, 5−50 μM) or *S*-nitroso-*N*-acetyl-D,L-penicillamine (SNAP, 50−100 μM) in the reaction mixture had no effect on 5α-OOH decay (suggesting that iron was not redox-inhibited) but slowed TBARS and 7αβ-OOH accumulation in a strongly dose-dependent fashion. Decomposed SPNO or SNAP had no such effects, implying that •NO was the responsible agent. Accumulation of several [^{14}C]Ch oxidation products, detected by high-performance thin-layer chromatography with phosphorimaging, was similarly diminished by active SPNO or SNAP. Concomitantly, a new band referred to as RCh.4 appeared, the radioactivity of which increased as a function of incubation time and •NO donor concentration. RCh.4 material was also generated via direct iron/ascorbate reduction of 7α-OOH in the presence of •NO, consistent with 7α-nitrite (7α-ONO) identity. However, various other lines of evidence suggest that RCh.4 is not 7α-ONO, but rather 5α-hydroxycholesterol (5α-OH) generated by reduction of 5α-ONO arising from 7α-ONO rearrangement. 5α-OH was only detected when •NO was present in the reaction system, thus providing indirect evidence for the existence of nitrosated Ch intermediates arising from •NO chain-breaking activity.

Nitric oxide (nitrogen monoxide, •NO) is a naturally occurring free radical gas that is involved in a wide range of physiological processes, including (i) induction of vasodilation and inhibition of platelet activation/adherence, (ii) neurotransmission in the central nervous system, and (iii) cytotoxic defensive mechanisms of neutrophils and macrophages (*1*−*3*). Nitric oxide is produced by a variety of mammalian cells that express •NO synthases, e.g., neuronal cells, endothelium, neutrophils, and macrophages. In keeping with its diverse biological functions, •NO is capable of playing a dual role in oxidative reactions, acting as a prooxidant on one hand and an antioxidant on the other, depending on the existing conditions (*4*, *5*). When generated in the presence of superoxide radical (O_2^-), with which it can react very rapidly ($k = 6.7 \times 10^9$ M^{-1} s^{-1}; *6*, *7*), •NO gives rise to peroxynitrite ($ONOO^-$)/peroxynitrous acid (ONOOH), a strong indiscriminate oxidant and nitrating agent that can modify lipids, proteins, and nucleic acids (*8*). On its own, however, •NO has been reported to protect cells against oxidative killing (*9*−*12*) and also to inhibit free radical-mediated lipid peroxidation in fatty acid micelles (*13*, *14*), liposomes (*15*, *16*), and low-density lipoprotein (*15*, *17*, *18*). Small organoperoxyl radicals in aqueous solution react rapidly with •NO ($k = 1-3 \times 10^9$ M^{-1} s^{-1}), giving rise to unstable peroxynitrite derivatives, which decompose to nitrogen dioxide radical, alkoxyl radicals, and alkyl nitrates (*19*). Similar interception of peroxyl radicals has been proposed to account for •NO's antiperoxidative effects in lipid systems (*13*−*18*). Although products of this reaction were not isolated for identification, they were reported to include alkyl nitrites, pernitrites, and nitrates on the basis of immediate, total product analysis by HPLC[1]−mass spectrometry (*13*, *15*). In the present study, we used [^{14}C]-cholesterol (Ch) as a liposomal reporter lipid for sensitive in situ tracking of peroxidative chain reactions induced by iron/ascorbate decomposition of a nonradiolabeled, nonregenerable "priming" hydroperoxide (*20*). Structures of cholesterol-derived species (ChOX) that can signal the occurrence of such reactions are shown in Figure 1. Nitric oxide arising from the decomposition of spermine NONOate (SPNO) or *S*-nitroso-*N*-acetylpenicillamine (SNAP) was found to be a potent inhibitor of certain ChOX formation in liposomes. Its reactivity was accompanied by the formation of a new species, which was deduced to be a rearrangement/reduction product of a nitrosated Ch intermediate.

† This work was supported by USPHS Grants CA70823 and CA72630 from the National Cancer Institute (A.W.G.) and by KBN Grant 4P05A-068-16 (W.K.).

* To whom correspondence should be addressed: telephone 414-456-8432; fax 414-456-6510; e-mail agirotti@mcw.edu.

‡ Jagiellonian University.

§ Medical College of Wisconsin.

10.1021/bi000393e CCC: $19.00
Published on Web 05/16/2000

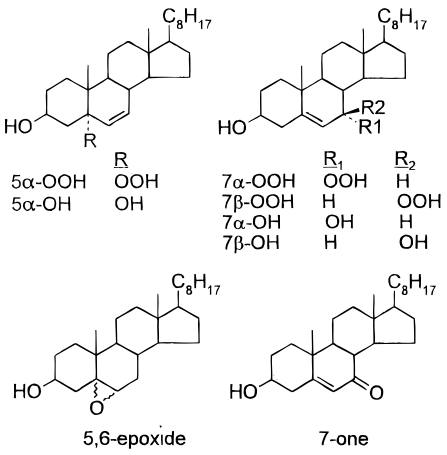

FIGURE 1: Structures of relevant cholesterol oxidation products: 3β-hydroxy-5α-cholest-6-ene-5-hydroperoxide (5α-OOH); 5α-cholest-6-ene-3β,5-diol (5α-OH); 3β-hydroxycholest-5-ene-7α-hydroperoxide (7α-OOH); 3β-hydroxycholest-5-ene-7β-hydroperoxide (7β-OOH); cholest-5-ene-3β,7α-diol (7α-OH); cholest-5-ene-3β,7β-diol (7β-OH); unspecified mixture of 5,6α-epoxy-5α- and 5,6β-epoxy-5β-cholestan-3β-ol (5,6-epoxide); and 3β-hydroxycholest-5-en-7-one (7-one).

EXPERIMENTAL PROCEDURES

Chemicals and Reagents. Sigma Chemical Co. (St. Louis, MO) supplied the following: cholesterol (Ch), Chelex-100 (50−100 mesh), 8-hydroxyquinoline, ascorbic acid, 2,6-di-*tert*-butyl-4-methylphenol (BHT), 3,5-di-*tert*-butyltoluene (DBT), and 2-thiobarbituric acid (TBA). *S*-Nitroso-*N*-acetyl-D,L-penicillamine (SNAP) and *N*-[4-[1-(3-aminopropyl)-2-hydroxy-2-nitrosohydrazino]butyl]-1,3-propanediamine (spermine NONOate, SPNO) were obtained from Cayman Chemical (Ann Arbor, MI) and used without further purification. [4-^{14}C]Cholesterol (50−60 mCi/mmol in toluene) was supplied by Amersham Life Sciences, Inc. (Arlington Heights, IL). 1,2-Dimyristoyl-*sn*-glycero-3-phosphocholine (DMPC), 1-palmitoyl-2-oleoyl-*sn*-glycero-3-phosphocholine (POPC), and egg yolk L-α-phosphatidylcholine (egg PC) were from Avanti Polar Lipids (Birmingham, AL). All chromatographic separations were carried out with HPLC-grade solvents obtained from Burdick and Jackson Corp. (Muskegon, MI). 3β-Hydroxy-5α-cholest-6-ene-5-hydroperoxide (5α-OOH), a singlet oxygen ($^1O_2$) adduct of Ch (*21*, *22*), was prepared by dye-sensitized photooxidation of Ch in pyridine solution (*22*, *23*). 5α-OOH was isolated from other reaction products by means of reverse-phase HPLC, and its identity was confirmed by proton NMR (*21*, *22*). In 2-propanol solution, 5α-OOH was stable for several months when stored at −20 °C; its concentration was determined by iodometric assay, as described (*24*, *25*). Authentic 5α-cholest-6-ene-3β,5-diol (5α-OH) was supplied by Dr. J. I. Teng (University of Texas, Galveston) as a gift. The α- and β-epimers of cholestan-5,6-epoxy-3β-ol (5,6-epoxide), used as HPTLC standards, were from Steraloids, Inc. (Wilton, NH). Also used as HPTLC standards, ^{14}C-labeled 3β-hydroxycholest-5-ene-7α-hydroperoxide (7α-OOH), 3β-hydroxycholest-5-ene-7β-hydroperoxide (7β-OOH), cholest-5-ene-3β,7α-diol (7α-OH), and cholest-5-ene-3β,7β-diol (7β-OH) were prepared as described (*26*). Stock 1.0 mM ferric-8-hydroxyquinoline [Fe(HQ)$_3$] was prepared by mixing 1.0 mM $FeCl_3$ in 4.0 mM HCl with 3.0 mM 8-hydroxyquinoline in 50% ethanol. Stock solutions of 5 mM SPNO in 0.1 M sodium phosphate (pH 8.5) were stored at −80 °C. Under these conditions, the SPNO was stable for indefinite periods; however, under experimental conditions (pH 7.4, 37 °C) its absorbance at 252 nm decayed with a $t_{1/2}$ of ∼38 min, in agreement with a reported value (*27*). Decomposed SPNO was prepared by acidifying a stock sample to pH 3−4. Stock solutions of 10 mM SNAP in dimethyl sulfoxide were prepared 5−10 min before use in an experiment and were essentially stable over this period. Stock solutions that had stood at room temperature in ambient light for 3−4 days were used as decomposed SNAP. In the presence of experimental liposomes, AH^-, and Fe(HQ)$_3$ at pH 7.4 and 37 °C, SNAP's absorbance at 340 nm decayed with a $t_{1/2}$ of ∼1 min. All aqueous solutions were prepared with deionized, glass-distilled water.

Preparation of Liposomes. Before incorporation into liposomal membranes, [^{14}C]Ch (∼1.5 μCi) plus unlabeled carrier (∼0.3 mg of total Ch) was separated from any preexisting oxidation products by means of normal-phase HPLC (*23*). The Ch fraction (detected by UV absorption at 212 nm) was recovered, dried under N_2, and used immediately. A chloroform solution containing egg PC or POPC, [^{14}C]Ch, and 5α-OOH in appropriate concentrations was dried under N_2 and then under vacuum. After hydration of the lipid film in PBS, followed by five cycles of freezing and thawing, the resulting multilamellar vesicles were passed through two 0.1 μm polycarbonate filters (Nucleopore Corp., Pleasanton, CA) in an Extruder apparatus (Lipex Biomembranes, Vancouver, BC) (*23*, *28*). The resulting unilamellar vesicles (LUVs), typically consisting of 1.0 mM egg PC or POPC, 0.75 mM (0.4−0.5 μCi/ml) [^{14}C]Ch, and 50 μM 5α-OOH in bulk-phase PBS, were stored under argon at 4 °C until used. The PBS used for these preparations was pretreated with Chelex-100 in order to deplete redox metal ions that might catalyze premature decomposition of 5α-OOH (*29*). Control LUVs lacking 5α-OOH consisted of 1.0 mM PC and 0.8 mM [^{14}C]Ch. The PC/Ch mole ratio of ∼1.3 in these preparations approximates that of most eukaryotic plasma membranes (*30*).

Experimental Conditions. Reaction systems at 37 °C were typically set up as follows. 5α-OOH-containing LUVs (1.8

[1] Abbreviations: ChOX, cholesterol oxidation (products/intermediates); AH^-, ascorbate; Ch, cholest-5-en-3β-ol (cholesterol); ChOOH, cholesterol hydroperoxide; EI-MS, electron impact mass specrometry; Fe(HQ)$_3$, ferric-8-hydroxyquinoline; BHT, butylated hydroxytoluene; DBT, 3,5-di-*tert*-butyltoluene; HPLC-EC(Hg), high-performance liquid chromatography with mercury cathode electrochemical detection; HPLC-RC, high-performance liquid chromatography with radiochemical detection; HPTLC-PI, high-performance thin-layer chromatography with phosphorimaging detection; LOOH, lipid hydroperoxide; LUV, large unilamellar vesicle; PBS, Chelex-treated phosphate-buffered saline (125 mM NaCl and 25 mM sodium phosphate, pH 7.4); PC, phosphatidylcholine; DMPC, 1,2-dimyristoyl-*sn*-glycero-3-phosphocholine; POPC, 1-palmitoyl-2-oleoyl-*sn*-glycero-3-phosphocholine; TBARS, thiobarbituric acid-reactive species; SNAP, *S*-nitrosyl-*N*-acetyl-D,L-penicillamine; SPNO, *N*-[4-[1-(3-aminopropyl)-2-hydroxy-2-nitrosohydrazino]butyl]-1,3-propanediamine (spermine NONOate); 5α-OOH, 3β-hydroxy-5α-cholest-6-ene-5-hydroperoxide; 5α-OH, 5α-cholest-6-ene-3β,5-diol; 5α-ONO, 3β-hydroxy-5α-*O*-nitrosocholest-6-ene; 5,6-epoxide, unspecified mixture of cholestan-5α,6α-epoxy-3β-ol and cholestan-5β,6β-epoxy-3β-ol; 7α-OOH, 3β-hydroxycholest-5-ene-7α-hydroperoxide; 7α-OH, cholest-5-ene-3β,7α-diol; 7α-ONO, 3β-hydroxy-7α-*O*-nitrosocholest-5-ene; 7β-OOH, 3β-hydroxycholest-5-ene-7β-hydroperoxide; 7β-OH, cholest-5-ene-3β,7β-diol; RCh.4, material with high-performance thin-layer chromatographic mobility ∼0.4 relative to cholesterol; 7-one, 3β-hydroxycholest-5-en-7-one.

mM total lipid in PBS) were enriched in redox-active iron by preincubating with 1.0 μM $Fe(HQ)_3$ for 15 min (*31*). Ascorbate (AH^-, 1.0 mM) was then introduced in order to trigger chain peroxidation via iron-mediated reduction of 5α-OOH. The AH^- was obtained from a stock solution of 0.1 M ascorbic acid in PBS, which was prepared immediately before an experiment (*20*). AH^- was either added alone or together with SPNO or SNAP at various starting concentrations in the 5−100 μM range. At various time points during the incubation of egg PC-containing LUVs, 200 μL samples were removed for TBA assay. In the case of POPC-containing LUVs, 50 μL samples were placed in polypropylene microfuge tubes, mixed with 5 μL of 5 mM EDTA and 0.2 mL of PBS, and then extracted with 0.4 mL of cold chloroform/methanol (2:1 v/v), as described (*24*, *25*). After separation of phases by centrifugation, a 0.2 mL aliquot from each organic phase was recovered for HPTLC-PI analysis and a 20 μL aliquot for HPLC-EC(Hg) analysis (see below). These samples were dried under N_2 and either chromatographed immediately or after being stored at −20 °C. Analyte signal intensities remained unchanged after 2−3 weeks of storage at −20 °C. Control mixtures lacking either $Fe(HQ)_3$ or AH^- or containing decomposed SPNO or SNAP were incubated and analyzed concurrently with experimental systems.

Thiobarbituric Acid Assay. Aldehyde byproducts arising from free radical peroxidation of liposomal egg PC were determined by TBA assay. [This could not be used for POPC LUVs because monoenoic fatty acyl groups do not produce TBARS (*32*).] A modified procedure with greatly improved sensitivity for small samples was used (*33*). A 200 μL sample from a liposome suspension was mixed with 5 μL of 0.5 mM butylated hydroxytoluene, 50 μL of 5% (w/v) trichloroacetic acid, and 50 μL of prewarmed 1.65% (w/v) 2-thiobarbituric acid. The mixture was heated at 100 °C for 15 min and cooled rapidly to room temperature, and the absorbance at 532 nm was recorded on a Hewlett-Packard diode-array spectrophotometer equipped with a 50 μL microcell. Absorbance readings were converted to thiobarbituric acid-reactive species (TBARS) levels by use of an extinction coefficient of 157 mM^{-1} cm^{-1} (*33*).

Thin-Layer Chromatography. Liposomal extracts containing [^{14}C]ChOX species were analyzed by high-performance thin-layer chromatography with phosphorimaging detection (HPTLC-PI) (*20*). Assignments were based on positions of [^{14}C]standards, which were run alongside. High-performance silica gel-60 plates (10 × 10 cm; 0.2 mm layer thickness) were supplied by EM Science (Gibbstown, NJ). Samples in hexane/2-propanol (97:3 v/v) were typically applied to a plate in a hairline N_2 stream, with a programmable Linomat IV dispenser from Camag Scientific Inc. (Wilmington, NC). Chromatography was carried out in a 9 × 20 × 24 cm glass chamber, with benzene/ethyl acetate (1:1 v/v) as the mobile phase. The average running time at 25 °C was 8 min. All operations were carried out under minimal room lighting to avoid any possible photodecomposition of •NO adducts (*34*). After air-drying, the plate was analyzed for ChOX species (including 7α-OOH, 7β-OOH, 5,6-epoxide, 7α-OH, and 7β-OH), using a Storm 860 storage phosphor system (*35*) with ImageQuant 4.2 software (Molecular Dynamics, Sunnyvale, CA). A 1−2 day development period at room temperature was typical. However, when subsequent examination of a temperature-sensitive species such as a putative •NO adduct was planned, the plate was developed at 4 °C and for the shortest possible time that allowed analyte detection. For the indicated specific radioactivity of liposomal [^{14}C]Ch (see above), the detection limit for an analyte such as 7α-OH or 7β-OH was determined to be ∼5 pmol. Well-resolved parent Ch (which was depleted by < 5% after a 45 min reaction) was used as an internal standard to correct for any discrepancies in sample loading. Determination of molar yields of the various analytes was based on the their image intensities relative to Ch and the absolute molar amount of Ch incorporated into the liposomes.

Column Chromatography. Reverse-phase high-performance liquid chromatography with mercury cathode electrochemnical detection [HPLC-EC(Hg)] can be used for highly sensitive and specific analysis of lipid hydroperoxides (LOOHs) (*26*, *36*, *37*). Alcohol analogues and other non-peroxide species generated during chain peroxidation are not detected by this approach. In this study, HPLC-EC(Hg) was used for monitoring the reductive decay of 5α-OOH, a singlet oxygen adduct of Ch (*22*), and concurrent accumulation of free radical-derived 7α- and 7β-OOH (*38*). These epimers are not resolvable under the conditions used and are thus referred to collectively as 7αβ-OOH. Chromatography was carried out using an Ultrasphere XL-ODS column (4.6 × 70 mm; 3 μm particles) from Beckman Instruments (San Ramon, CA), a Model 2350 HPLC pump with injection valve from Isco (Lincoln, NE), and a Model 420 electrochemical detector from EG&G Instruments, Inc. (Oak Ridge, TN). The detector is equipped with a renewable mercury drop electrode, which was set to operate at −150 mV vs a Ag/AgCl reference. Separations were carried using a deoxygenated mobile phase composed of (by volume) 72% methanol, 11% acetonitrile, 8% 2-propanol, and 9% aqueous solution containing 1 mM sodium perchlorate and 10 mM ammonium acetate. The elution flow rate was typically 1.5 mL/min. Lipid extracts in 2-propanol were injected manually through a 10 μL loop in the injection valve. The detection limits for 7αβ-OOH and 5α-OOH, which are equally EC-responsive, are approximately 0.1 and 0.2 pmol, respectively (*37*). Other details were as described (*36*, *37*).

Normal-phase high-performance liquid chromatography with radiochemical detection (HPLC-RC) was used in addition to HPTLC-PI for analyzing [^{14}C]ChOX species. Chromatography was carried out using a silica gel column (4.6 × 250 mm; 5 μm particles) and a mobile phase consisting of (by volume) 97% hexane and 3% 2-propanol. Elution rate was typically 1.2 mL/min. ^{14}C-Labeled analytes were detected with a Radiomatic A100 Flow-One\Beta detector equipped with a 0.5 mL flow cell (Radiomatic Instruments, Tampa, FL).

Mass Spectrometry. EI-MS analyses of sterol samples were carried out using a Hewlett-Packard 5985B mass spectrometer (Palo Alto, CA) equipped with a temperature-programmable direct insertion probe (DIP) and ChemStation software. The sample was typically dissolved in 10 μL of methanol, drawn up into the tip of a standard open-ended capillary tube, and allowed to air-dry into a thin film. A 6-mm length of capillary with deposited sample was placed into the DIP nest, which in turn was inserted, via vacuum interlock, directly into the mass spectrometer ion source. Temperature was programmed to cover the 50−330 °C range

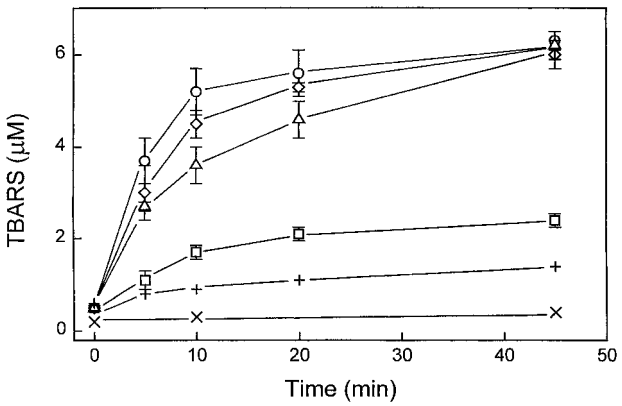

FIGURE 2: Effects of SPNO on generation of thiobarbituric acid-reactive species (TBARS) in iron/ascorbate-treated liposomes. Unilamellar LUVs (1.0 mM egg PC/0.75 mM Ch/0.05 mM 5α-OOH) in PBS were treated with 1.0 mM AH^- alone (×) and with 1.0 μM $Fe(HQ)_3$/1.0 mM AH^- without (○) or with 5 μM SPNO (△), 50 μM SPNO (□), or 50 μM decomposed SPNO (◇). Other liposomes lacking 5α-OOH (1 mM egg PC/0.8 mM Ch) were treated with $Fe(HQ)_3/AH^-$ only (+). At the indicated time points during incubation at 37 °C, samples were removed for TBARS determination. Data points are means of duplicate experimental values and represent TBARS levels in the reaction mixtures.

at 30 °C/min. Mass spectral data were acquired by electron impact (EI) ionization in a mass range of 50−500 amu.

RESULTS

Effects of an •NO Donor on TBA-Detectable Lipid Peroxidation. As evidenced by TBA assay, egg PC/Ch/5α-OOH (20:15:1 mol/mol/mol) LUVs in demetalled PBS underwent a burst of free radical-mediated lipid peroxidation when exposed to 1.0 μM $Fe(HQ)_3$ and 1.0 mM AH^- (Figure 2). The net TBARS content increased rapidly to ∼5 nmol/mL after 10 min and changed relatively slowly thereafter. As observed previously with other systems (*20*, *33*), no reaction occurred when $Fe(HQ)_3$ was omitted, indicating that the concentration of endogenous redox iron was vanishingly small in this system and that AH^- alone was insufficient to drive the reaction. Similarly, and in agreement with previous findings (*33*), there was no reaction when AH^- was omitted, indicating that continuous iron reduction was necessary. When membranes lacking 5α-OOH, i.e., egg PC/Ch (20:16 mol/mol) LUVs, were exposed to $Fe(HQ)_3/AH^-$, the maximal TBARS yield was much lower (∼10% of that with 5α-OOH present; Figure 2), suggesting that 5α-OOH was the most important "primer" of chain peroxidation reactions (*32*, *39*). The small reaction observed without 5α-OOH is attributed to a low level of preexisting hydroperoxide in the egg PC. Adding SPNO simultaneously with AH^- to the egg PC/Ch/5α-OOH incubation mixture resulted in a dose-dependent diminution of TBARS formation over the 5−50 μM SPNO range (Figure 2). However, decomposed SPNO (50 μM) had barely any inhibitory activity, implying that SPNO-derived •NO was responsible for the effects described (Figure 2).

Effects of •NO Donors on 5α-OOH Decay and 7αβ-OOH Appearance. Nitric oxide may inhibit chain peroxidation by (i) ligating and thus incapacitating Fe(II) or Cu(I) involved in one-electron turnover of chain-initiating hydroperoxides (*5*, *40*) or (ii) intercepting chain-carrying free radical intermediates (*13*−*18*). From TBARS results alone (Figure 2), one cannot determine which of these two alternatives is more important. To address this question and at the same time acquire information about Ch participation in the peroxidative process, we used HPLC-EC(Hg) to monitor loss of 5α-OOH (the priming hydroperoxide) on one hand and accumulation of 7αβ-OOH (free radical-derived hydroperoxides) on the other. For most of the initial experiments along these lines, liposomes were prepared from a relatively simple monoenoic phospholipid, POPC, instead of egg PC. As shown in Figure 3A, 5α-OOH in POPC/[^{14}C]Ch/5α-OOH (20:15:1 mol/mol/mol) LUVs decayed in apparent first-order fashion during incubation with $Fe(HQ)_3$ and AH^- ($k \sim 0.077$ min^{-1}; initial rate ∼ 3.8 μM/min). Concurrently, there was a rapid accumulation of 7αβ-OOH (Figure 3B), which reached an apparent steady state after 20−30 min and then declined. Neither of these changes in peroxide level was observed when AH^- was added without $Fe(HQ)_3$ (Figure 3), which is consistent with the results shown in Figure 2. Similarly, $Fe(HQ)_3$ without AH^- was without effect (not shown). Whereas SPNO at a starting concentration up to 50 μM had no obvious effect on 5α-OOH decay (Figure 3A), it had a striking suppressive effect on 7αβ-OOH, reducing the steady-state level and the time to reach this level in a dose-dependent fashion (Figure 3B). Failure of 50 μM SPNO to slow 5α-OOH decay rules out iron ligation (either by active/spent donor or by liberated •NO) as a possible explanation for diminished 7αβ-OOH accumulation. A progressive slowdown became apparent at SPNO concentrations greater than 100 μM (not shown), indicating that interference with iron redox cycling was possible if •NO fluxes were high enough. The observed inhibitory effects of <100 μM SPNO are attributed to •NO interception of oxyl or peroxyl radicals derived either from one-electron reduction of 5α-OOH or from downstream lipid targets, including

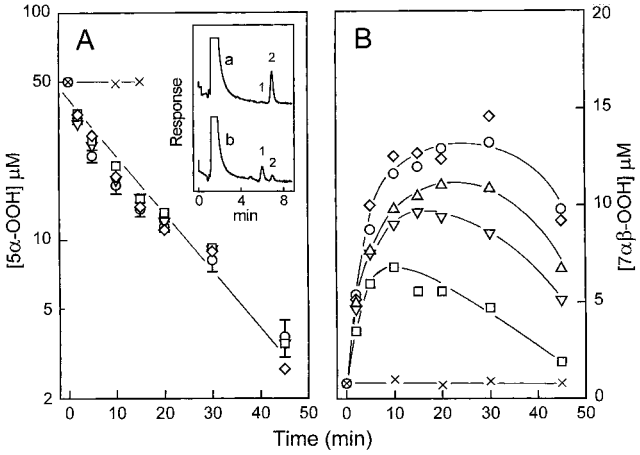

FIGURE 3: Effects of SPNO on 5α-OOH decay and 7αβ-OOH appearance. Liposomes consisting of 1.0 mM POPC, 0.75 mM (0.4 μCi/mL) [^{14}C]Ch, and 0.05 mM 5α-OOH in PBS were treated with 1.0 mM AH^- alone (×) and with 1.0 μM $Fe(HQ)_3$/1.0 mM AH^- without (○) or with SPNO: 5 μM (△), 20 μM (▽), 50 μM (□), or 50 μM decomposed SPNO (◇). After the indicated periods of incubation at 37 °C, lipids were extracted and analyzed by HPLC-EC(Hg). Each injected sample contained ∼3.3 nmol of total lipid. (A) Time courses for 5α-OOH decay; data points are means ± SD of values from three replicate experiments. (Inset) Peroxide profiles before (a) and after (b) incubation with $Fe(HQ)_3/AH^-$ for 45 min; 7αβ-OOH (peak 1) and 5α-OOH (peak 2). (B) Time courses for 7αβ-OOH accumulation; data are from one of the experiments represented in panel A. Plotted values represent peroxide levels in reaction mixtures.

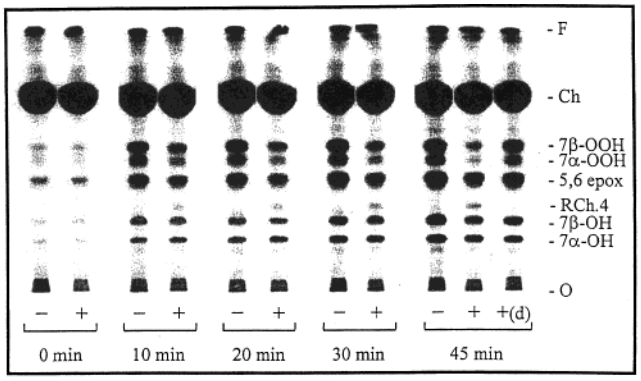

FIGURE 4: Thin-layer chromatogram showing effects of SPNO on formation of [^{14}C]ChOX species. Samples were from one of the experiments described in Figure 3. The 5α-OOH-containing LUVs were treated with $Fe(HQ)_3/AH^-$ in the absence of SPNO (−), presence of 50 μM SPNO (+), or presence of 50 μM decomposed SPNO [+(d)]. At the indicated times, lipids were extracted and chromatographed on a silica gel HPTLC plate, with benzene/ethyl acetate (1:1 v/v) as the mobile phase; O, origin; F, solvent front. Running time was ~8 min. After separation, radiolabeled species were detected and quantified by phosphorimaging autoradiography. Assignment of known ChOX species (7α-OOH, 7β-OOH, 5,6-epoxide, 7α-OH, 7β-OH) was based on location of authentic standards run separately or in spiked experimental samples. RCh.4 represents a product of mobility ~0.4 relative to Ch. Sample load per lane was ~60 nmol of total lipid (~10 nCi of total radioactivity).

POPC and Ch. Interception at the former level would prevent chain reactions from being initiated, whereas interception at the latter level would result in chain breaking/shortening. Chain-breaking activity is assumed to have played an important role in the •NO effects described because the SPNO half-life (38 min) was sufficiently long relative to the steady-state time for 7αβ-OOH (Figure 3B).

Overall ChOX Formation in the Absence and Presence of •NO Donors. To further explore the antiperoxidative effects of SPNO-derived •NO, and at the same time look for the possible existence of •NO-lipid adducts, we made use of a novel TLC approach that was recently developed in this laboratory (*20*). The approach is based on incorporation of a radiolabeled "reporter" lipid, e.g., [^{14}C]Ch, into a target membrane and determining the various oxidized species that derive from this lipid when a nonlabeled priming hydroperoxide such as 5α-OOH undergoes one-electron turnover. When [^{14}C]Ch is used, oxidized intermediates/products called ChOX species are analyzed by high-performance thin-layer chromatography with phosphorimaging detection (HPTLC-PI). Figure 4 shows results from a representative experiment with POPC/[^{14}C]Ch/5α-OOH LUVs. Before incubation with $Fe(HQ)_3/AH^-$, essentially all of the radioactivity (>99%) was found in Ch. During incubation, a group of [^{14}C]ChOX appeared, including 7α-OOH, 7β-OOH, 7α-OH, 7β-OH, and 5,6-epoxide, which collectively accounted for 3−4% of the total radioactivity after 45 min. Consistent with earlier findings (*20*), no 7-ketone (7-one) was apparent, which is surprising because this has been reported to be a major product of Ch autoxidation (*38*). If any 7-one was present, it might have been obscured by 5,6-epoxide, which migrates slightly ahead of it. Whereas 7α-OOH and 7β-OOH could not be resolved from one another by reverse-phase HPLC, they were readily resolved by normal-phase HPTLC (Figure 4). At a starting concentration of 50 μM, SPNO reduced the time-dependent buildup not only of 7α-OOH and 7β-OOH (in agreement with the Figure 3B data) but also of nonperoxide ChOX such as 5,6-epoxide. By contrast, decomposed SPNO (represented only at 45 min in Figure 4) had little or no effect. These results, like the others described, are consistent with the notion that •NO can inhibit lipid peroxidation by intercepting propagating radicals, including Ch-derived radicals. ChOX suppression by SPNO was accompanied by the appearance of a new band called RCh.4 (mobility ~0.4 relative to Ch), which consistently migrated between 7β-OH and 5,6-epoxide (Figure 4). The amount of RCh.4 material increased over time, but none of it was seen when decomposed SPNO was used, suggesting that it might represent some type of •NO adduct or product thereof.

Time course plots for accumulation of the various ChOX species seen in Figure 4 are shown in Figure 5. Among these species, 7α-OOH and 7β-OOH (like 5α-OOH) are susceptible to one-electron reduction, making them reactive intermediates, whereas 5,6-epoxide, 7α-OH, and 7β-OH are stable products, at least under the conditions used. Consistent with this and in agreement with previous findings (*20*), 7α-OOH and 7β-OOH levels in the basal reaction system increased to an apparent steady state after ~30 min and then gradually declined. The steady level of 7β-OOH was about twice that of 7α-OOH (Figure 5), possibly reflecting equilibration in favor of the more stable β-epimer (*41*). The kinetic profiles of 7α- and 7β-OOH, and their combined upper limit (~14 μM after 30 min), were similar to those determined by HPLC-EC(Hg) (Figure 3B), which reflects favorably on the accuracy of the two different analytical methods used. In contrast to the 7-hydroperoxides, 7α-OH and 7β-OH accumulated linearly over time, and at about the same rate (Figure 5). The latter suggests that precursor 7α-OOH and 7β-OOH levels were also the same in situ, but shifted in favor of the β-epimer during sample preparation, i.e., lipid extraction and solvent evaporation. In agreement with HPLC-EC(Hg) findings (Figure 3B), SPNO (but not spent SPNO) reduced the steady-state time and concentration of HPTLC-PI-assessed 7α-OOH and 7β-OOH in a dose-dependent fashion (Figure 5). At a donor concentration of 50 μM, the peak level of each epimer was lowered by 65%, and after 45 min barely any of each was detectable. SPNO appeared to have no significant effect on 7α-OH or 7β-OH formation over a 45 min period. It did slow 5,6-epoxide formation, but this only became obvious after ~10 min. As also shown in Figure 5, RCh.4 material accumulated in a time- and SPNO dose-dependent manner, reaching an upper level of 1.2 μM (~0.2% of the starting [Ch]) after 45 min. Initial rates determined from plots such as shown in Figure 5 are listed in Table 1. Note that SPNO had little, if any, diminishing effect on the 7α-OOH and 7β-OOH initial rates despite the fact that it lowered their steady-state concentrations. Similarly, SPNO had no effect on the 5,6-epoxide, 7α-OH, and 7β-OH initial rates. Also shown in Table 1 are values for experiments in which SNAP was used as the •NO donor (system 2). Unlike SPNO, SNAP slowed the initial accumulation of all ChOX analytes. Concomitantly, a chromatographic band with the mobility characteristics of RCh.4 appeared (Table 1). Observing RCh.4 material with two structurally distinct donors argues against the remote possibility that this material derived from the active or decomposed donor rather than from emitted •NO.

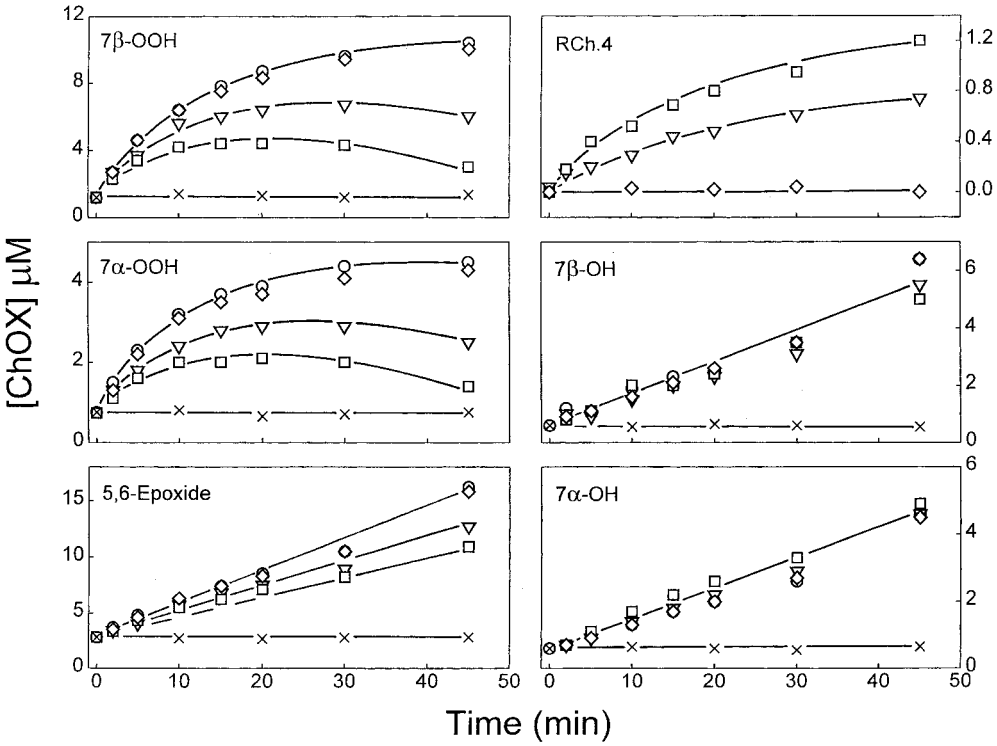

FIGURE 5: Time courses for the accumulation of various [^{14}C]ChOX species detected by HPTLC-PI. The data are from a single experiment, which is representative of at least three carried out under the same experimental conditions (see Figures 3 and 4). Liposome treatments were as follows: AH^- alone (×); $Fe(HQ)_3/AH^-$ (○); and $Fe(HQ)_3/AH^-$ plus 20 μM SPNO (▽), 50 μM SPNO (□), or 50 μM decomposed SPNO (◇). Plotted values represent ChOX levels in the liposome suspensions.

Table 1: Rates of ChOX Accumulation in Peroxide-Primed Liposomes: Effects of •NO Donors

additions to basal system	initial rate [nmol/(mL·min)][a]					
	5,6-epoxde	7α-OOH	7β-OOH	7α-OH	7β-OH	RCh.4
			System 1[b]			
none	0.38 ± 0.10	0.45 ± 0.15	0.73 ± 0.20	0.10 ± 0.02	0.13 ± 0.02	nd[e]
SPNO, 20 μM	0.37 ± 0.10	0.48 ± 0.10	0.71 ± 0.21	0.10 ± 0.01	0.12 ± 0.02	0.04 ± 0.01
SPNO, 50 μM	0.35 ± 0.15	0.45 ± 0.12	0.70 ± 0.23	0.10 ± 0.01	0.11 ± 0.01	0.08 ± 0.01
dec SPNO, 50 μM	0.37 ± 0.10	0.46 ± 0.15	0.75 ± 0.20	0.10 ± 0.02	0.15 ± 0.02	nd
			System 2[c]			
none	0.60 ± 0.10	0.90 ± 0.20	1.20 ± 0.20	0.20 ± 0.05	0.30 ± 0.05	nd
SNAP, 100 μM	0.05 ± 0.03	0.03 ± 0.02	0.03 ± 0.02	0.05 ± 0.03	0.03 ± 0.02	0.10 ± 0.05
dec SNAP, 100 μM	0.50 ± 0.10	1.00 ± 0.15	1.10 ± 0.20	0.20 ± 0.04	0.30 ± 0.06	nd
			System 3[d]			
none	na[f]	3.40 ± 0.20	na	3.50 ± 0.30	na	nd
SPNO, 100 μM	na	3.30 ± 0.20	na	3.00 ± 0.30	na	0.48 ± 0.12

[a] Average values from duplicate experiments are shown; for system 1, one of these experiments is represented in Figure 5. [b] System 1 consisted of POPC/[^{14}C]Ch/5α-OOH (20:15:1, mol/mol/mol) LUVs at 1.8 mM total lipid, 1.0 μM $Fe(HQ)_3$, and 1.0 mM AH^- in PBS at 37 °C. Reactions were started with AH^-, which was added either alone or together with active or decomposed SPNO at the indicated concentrations. Timed samples were extracted and [^{14}C]ChOX levels in lipid fractions were determined by HPTLC-PI. [c] System 2 was identical to system 1 except for the use of active and decomposed SNAP instead of SPNO. [d] System 3 consisted of DMPC/[^{14}C]7α-OOH (9:1 mol/mol) LUVs at 0.33 mM total lipid, 1.0 μM $Fe(HQ)_3$, and 1.0 mM AH^- in PBS at 37 °C. Where indicated, SPNO was included from the outset. The 7α-OOH rate in this system reflects a decay rather than an accumulation, as observed in systems 1 and 2. [e] nd, not detected. [f] na, not applicable because chain reactions were not monitored in this system.

Comparative Effects of •NO and BHT. The observed effects of •NO on most, but not all, ChOX species prompted us to ask how these results would compare with those obtained with BHT, a classic chain-breaking antioxidant (*42*). As shown in Table 2, 25 μM BHT substantially decreased the rate of accumulation of all free radical-derived ChOX, including 7α-OH and 7β-OH. By contrast, DBT, a nonhydroxylated BHT analogue used as a control, had no significant effect on any of the analytes. This rules out the possibility of nonspecificity on the part of BHT, i.e., effects not related to free radical scavenging. At the concentration used, BHT had no effect on 5α-OOH decay (results not shown), confirming that it interfered with chain initiation/propagation rather than one-electron reduction of the primary hydroperoxide. Slow release of •NO from SPNO and different antioxidant mechanisms for •NO and BHT might explain why the latter caused a large diminution in the 7α- and 7β-OH rates (Table 2) while the former had no apparent effect (Figure 5). BHT quenches free radicals by hydrogen abstraction (*42*, *43*), whereas •NO appears to do so by direct addition (*13*, *14*). Some •NO adducts might rapidly decompose to final products observed in the absence of •NO. If this occurred in

Table 2: Effects of a Phenolic Antioxidant on Rates of ChOX Accumulation in 5α-OOH-Primed Liposomes

additions to basal system[a]	initial rate [nmol/(mL·min)]				
	5,6-epoxide	7α-OOH	7β-OOH	7α-OH	7β-OH
none	0.35 ± 0.01	0.55 ± 0.10	0.95 ± 0.12	0.16 ± 0.01	0.20 ± 0.01
BHT, 25 μM	0.11 ± 0.01	0.10 ± 0.05	0.33 ± 0.05	0.06 ± 0.01	0.08 ± 0.01
DBT, 25 μM	0.36 ± 0.03	0.47 ± 0.04	1.00 ± 0.10	0.16 ± 0.01	0.21 ± 0.01

[a] The basal reaction system contained POPC/[^{14}C]Ch/5α-OOH LUVs (1.8 mM total lipid), 1.0 μM $Fe(HQ)_3$, and 1.0 mM AH^- in PBS at 37 °C. The membranes were preincubated with $Fe(HQ)_3$ in the absence or presence of BHT or DBT for 15 min before introduction of AH^-. Samples at various time points were extracted and [^{14}C]ChOX levels in lipid fractions were determined by HPTLC-PI. Values shown are from duplicate experiments.

our system, it could account (at least in part) for the observed lack of effect of SPNO-derived •NO on 7α- and 7β-OH accumulation.

Characterization of Material in the RCh.4 Band. Radiolabeling (Figure 4) specifies that RCh.4 was derived from Ch. Knowing that 7-peroxyl and 7-oxyl radicals are prominent intermediates in iron-catalyzed Ch peroxidation (*38*, *39*), and that •NO reacts rapidly with radicals of this type (*19*, *44*), we postulated that RCh.4 might be a product of one of these reactions. A nitrosated (or nitrated) species [7-ONO(O)] was considered to be the most likely candidate. Reaction of N_2O_4 with organoperoxides (*45*) or •NO with peroxyl radical intermediates of autoxidizing lipids (*13*−*15*) has been reported to generate compounds of this type. Such compounds derive most likely from bond homolysis of unstable pernitrite (ROONO) intermediates, followed by dissociation or recombination of radical pairs (*45*). One approach that we used for determining whether RCh.4 might represent a 7-nitr(os)ated Ch derivative was to look for the appearance of RCh.4 material in DMPC/[^{14}C]7α-OOH LUVs exposed to $Fe(HQ)_3/AH^-$/SPNO. Since this system lacked Ch, [^{14}C]7α-OOH served as a nonregenerable hydroperoxide, and any RCh.4 that appeared could be directly linked to free radicals derived from this hydroperoxide. As shown in Table 1 (system 3), 7α-OOH decay was not affected by 100 μM SPNO, implying that redox iron in this system (like that in the 5α-OOH-primed system, Figures 3 and 4), was not constrained by •NO. The rate of 7α-OOH decay and corresponding accumulation of 7α-OH, its diol reduction product (3.5 μM/min), was comparable to that observed for 5α-OOH under similar reaction conditions (3.8 μM/min), which agrees with previous determinations (*20*). In the presence of SPNO and concurrent with the appearance of 7α-OH, there was a rapid accumulation of radioactive material with the same chromatographic mobility as RCh.4; a maximal level was reached after ∼10 min (Figure 6; Table 1, system 3). Competition of •NO with AH^- for 7α-O• in this experiment could account for the small (∼15%) decrease observed in the 7α-OH rate (Table 1, system 3). When the reaction was carried out with [^{14}C]7β-OOH instead of [^{14}C]7α-OOH, relatively little RCh.4 was generated (initial rate <5% of that with the 7α epimer) and no new bands were observed (Figure 6), suggesting that •NO reacted preferentially at the 7α position. (A likely explanation is that •NO attacking on the sterol β-face would have been sterically hindered by the bulky methyl group at the C-10 position.) These findings were at least consistent with RCh.4 being the 7α-*O*-nitroso derivative of Ch (7α-ONO).

However, other evidence appeared to be at odds with this conclusion. For example, RCh.4 was observed to have approximately the same mobility on HPTLC as 5α-hydroxy-

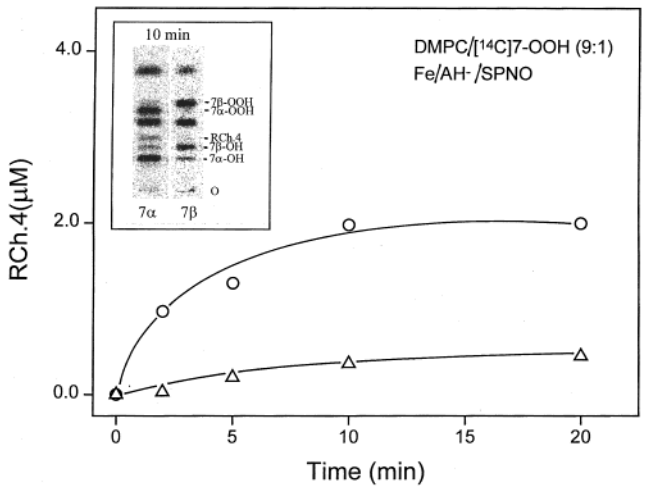

FIGURE 6: Time courses for the generation of RCh.4 material in liposomes containing radioactive 7α-OOH (○) or 7β-OOH (△) as the only redox-active lipid. A LUV suspension consisting of 300 μM DMPC and 33 μM (0.5 μCi/mL) [^{14}C]7α-OOH or [^{14}C]7β-OOH in PBS was incubated in the presence of 1.0 μM $Fe(HQ)_3$, 1.0 mM AH^-, and 100 μM SPNO at 37 °C. At the indicated time points, samples were removed and lipids extracted for HPTLC-PI analysis. Plotted values represent RCh.4 levels in the reaction mixtures. (Inset) HPTLC-PI profiles after a 10 min reaction period. Five [^{14}C]ChOX bands are assigned as indicated; the two remaining bands are undefined.

cholesterol (5α-OH), a $^1O_2$-derived species (*22*). It seemed unlikely at first that RCh.4 could be this diol because 5α-OOH was unlabeled when used as a priming hydroperoxide. Also, no [^{14}C]5α-OOH or [^{14}C]5α-OH could be detected when chain peroxidation was carried out in the absence of •NO (Figure 4), nor is there any known mechanism by which •NO can give rise to $^1O_2$ under these reaction conditions. To explore this further, we attempted to isolate RCh.4 from other [^{14}C]ChOX for further characterization. Initial attempts at doing this by means of preparative-scale HPTLC were unsatisfactory, largely because of difficulties in recovering the low yields of RCh.4 material from silica gel. Much better results were obtained with normal-phase HPLC with radiochemical detection. As shown in Figure 7 (trace I), 5α-OOH-primed LUVs displayed at least six [^{14}C]ChOX peaks after being treated with $Fe(HQ)_3/AH^-$ for 90 min at 37 °C. All of these, except the one immediately preceding Ch and the pair immediately after it (5.8 and 7.9 min) were assigned by use of [^{14}C]standards. Note that 5,6-epoxide and 7αβ-OOH migrated in the reverse order to that seen on HPTLC (Figure 4). When the reaction was carried out in the presence of 50 μM SPNO, peak 4 (representing 7αβ-OOH) was no longer detectable and all other ChOX peaks were substantially diminished (Figure 7, trace II), in qualitative agreement with the HPTLC-PI observations (Figure 4). Concomitantly, a new

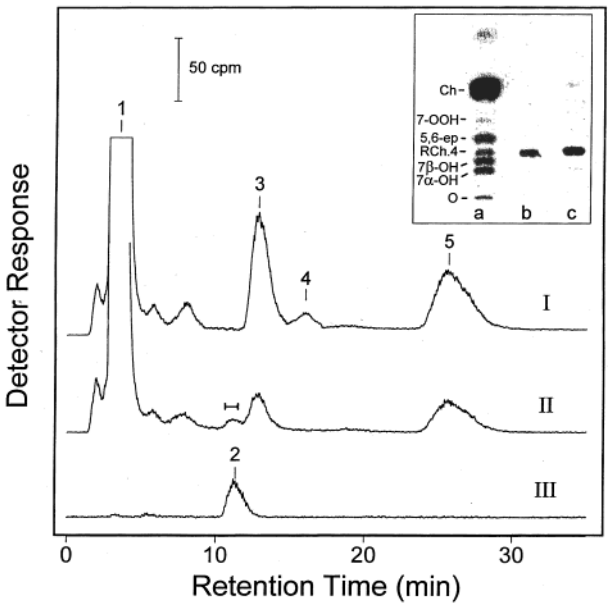

FIGURE 7: HPLC-RC profiles showing the effects of SPNO on the accumulation of various [^{14}C]ChOX species. LUV membranes containing 1.0 mM DMPC, 0.8 mM (5.0 μCi/mL) [^{14}C]Ch, and 0.05 mM 5α-OOH in bulk suspension in PBS were exposed to 1.0 μM Fe(HQ)$_3$ and 1.0 mM AH$^-$ in the absence and presence of 50 μM SPNO. After 90 min of incubation at 37 °C, lipids were extracted and subjected to HPLC-RC analysis. The chromatographic traces represent the following samples: (I) reaction system without SPNO; (II) reaction system with SPNO; (III) [^{14}C]5α-OH standard. Total lipid injected onto the column was as follows: (I) 138 nmol; (II) 138 nmol; (III) 10 nmol. Peak assignments are as follows: (1) Ch (3.4 min); (2) 5α-OH (11.3 min); (3) 5,6-epoxide (12.9 min); (4) 7αβ-OOH (16.0 min); (5) 7αβ-OH (25.5 min). (Inset) HPTLC-PI profiles representing (a) reaction system with SPNO; (b) 10.5−11.5 min fraction from HPLC-RC run II (indicated by bar); (c) [^{14}C]5α-OH standard. Total lipid analyzed was as follows: (a) 69 nmol; (b) ∼0.2 nmol; (c) ∼0.5 nmol.

peak was consistently observed slightly upstream of 5,6-epoxide (Figure 7, trace II). The retention time of this peak (11.3 min) was found to be identical to that of authentic 5α-OH (Figure 7, trace III) and the yield (∼0.2% of the total radioactivity) was in the same range as that of RCh.4 described in Figures 4 and 5. Material in the leading portion of the new peak (fraction indicated with bar in trace II) was recovered and analyzed by HPTLC-PI. As shown in the Figure 7 inset, this material (lane b) had the same relative mobility as RCh.4 in a whole extract from SPNO/iron/AH$^-$-treated LUVs (lane a) or authentic 5α-OH (lane c). Thus, using two independent techniques, we established that RCh.4 material had the same chromatographic properties as 5α-OH.

Additional examination of HPLC-RC-isolated RCh.4 by means of EI-MS revealed an ionization/fragmentation pattern that was entirely consistent with it being 5α-OH. Thus, RCh.4 gave a prominent molecular ion peak at *m*/*z* 402 ([M]$^+$) as well as fragmentation/rearrangement peaks at *m*/*z* 384 ([M − 18]$^+$) and *m*/*z* 351 [M − 51]$^+$) in relative abundance 4%, 57%, and 39%, respectively. Authentic 5α-OH analyzed under identical conditions gave peaks at *m*/*z* 402, 384, and 351 in relative abundance 5%, 55%, and 40%, respectively, which is consistent with published data (*46*). On the basis of all the evidence provided, therefore, we conclude that RCh.4 was in fact 5α-OH rather than a 7α-nitrosated species. The mechanism by which 5α-OH arose

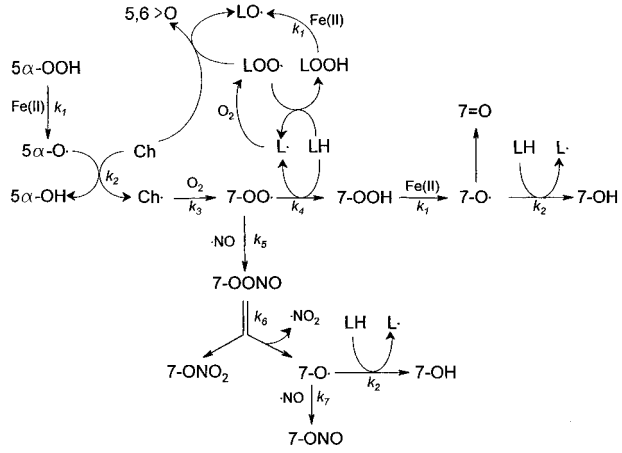

FIGURE 8: Reaction scheme for 5α-OOH-induced chain peroxidation, showing proposed sites of free radical interception by •NO. Only the key components of the various reactions are shown. Chain propagation reactions triggered by 7α- or 7β-peroxyl radical (7-OO•) are depicted, where LH represents an oxidizable lipid (either Ch or POPC). A similar wave of propagation from 7-O• (LO•) is omitted for the sake of clarity. Ch• represents the C7-centered cholesteryl radical; 5,6>O, cholesterol-5,6-epoxide; and 7=O, 7-ketocholesterol. Approximate rate constants for key reactions are as follows (with references in parentheses): k_1 ∼2 × 10^3 M^{-1} s^{-1} (*49*); k_2 ∼100−500 M^{-1} s^{-1} (*50*); k_3 ∼1 × 10^9 M^{-1} s^{-1} (*51*); k_4 ∼10−50 M^{-1} s^{-1} (*52*); k_5 ∼2 × 10^9 M^{-1} s^{-1} (*19*); k_6 ∼0.2 s^{-1} (*19*); k_7 ∼3 × 10^9 M^{-1} s^{-1} (*44*).

in the presence of •NO is not certain, but a reasonable possibility (to be elaborated upon in the Discussion) is that it derived from 5α-ONO arising from allylic rearrangement of 7α-ONO.

DISCUSSION

In this study we used unilamellar LUVs fabricated so as to model a slightly peroxidized eukaryotic plasma membrane, i.e., with a preexisting hydroperoxide content of 2−3 mol % based on total lipid. For most experiments, we used singlet oxygen- ($^1O_2$-) derived 5α-OOH (see Figure 1) as the preexisting hydroperoxide, which served as a primer of chain peroxidation reactions in the face of iron/AH$^-$ reductive pressure. A cytopathological connection for this model might be the exposure of skin fibroblasts to long-wave ultraviolet radiation (UVA), which has been reported to generate singlet oxygen and mobilize iron in such cells (*47*, *48*). As shown in Figure 8, one-electron reduction of 5α-OOH gives a free radical species that can induce a peroxidative chain by abstracting hydrogen from a contiguous unsaturated lipid, shown here as Ch. The initiating radical is depicted as 5α-oxyl (5α-O•), which gives rise to the diol 5α-OH. However, another possibility, suggested by findings with fatty acid-derived oxyl radicals (*53*, *54*), is the 5,6-epoxy-7-peroxyl radical formed by rapid allylic rearrangement of 5α-O• and O_2 addition. Preferential abstraction of an allylic H at the C7 position of Ch, followed by rapid O_2 addition, gives the 7α- or 7β-peroxyl radical (7-OO•). The latter serves as a propagating intermediate by dehydrogenating a neighboring lipid (LH), which could either be another Ch or a POPC molecule. Concomitantly, a 7-hydroperoxide (7-OOH) is formed, which, like 5α-OOH, is subject to one-electron turnover, giving rise sequentially to the 7α- or 7β-oxyl radical (7-O•) and thence to the corresponding diol (7-OH). In addition to propagating chains, 7-OO• and other peroxyl radicals may attack at the double bond of Ch (Figure 8),

converting it to the 5α,6α- or 5β,6β-epoxide (5,6>O) via −O−O− bond homolysis (*54*). Moreover, 7-O• may undergo β-scission of hydrogen at C7, resulting in 7-ketocholesterol (7=O) formation. 7α-OOH, 7β-OOH, 7α-OH, 7β-OH, 7-one, and 5,6-epoxide are the major ChOX species that derive from Ch autoxidation (*38*, *39*). Compared with molecular species generated by phospholipid autoxidation, these ChOX are relatively few in number and much easier to separate, not only from one another and parent Ch but also from other lipids. Three complementary techniques based on ChOX analysis, HPLC-EC(Hg), HPTLC-PI, and HPLC-RC, were used for monitoring chain peroxidation as described in Figure 8 and for assessing the effects of •NO on it. The first two of these were developed in this laboratory (*20*, *37*) and are among the most sensitive in existence for analyzing lipid peroxidation intermediates and products. The primary purpose of HPLC-EC(Hg) was for tracking Ch hydroperoxide status during reductive lipid peroxidation, i.e., the decay of 5α-OOH on one hand and appearance of free radical-derived 7αβ-OOH on the other. 5α-OOH turnover in iron/AH$^-$-treated LUVs was accompanied by POPC hydroperoxide formation (not shown) in addition to 7αβ-OOH formation. POPC hydroperoxides were well resolved from faster-eluting Ch hydroperoxides under the conditions used, but analysis of the former was difficult because of a 200-fold greater detection limit (*36*, *37*). The initial rates of 5α-OOH decay and 7αβ-OOH accumulation were unaffected by varying the AH$^-$ concentration from 0.5 to 2.0 mM but increased in direct proportion to the Fe(HQ)$_3$ concentration over the 0.2−1.0 μM range (*20*), indicating that iron was the rate-determining reactant in the chain initiation step (Figure 8). In agreement with this, increasing or decreasing the 5α-OOH content of LUVs by 50% had no significant effect on these rates (data not shown). We consistently found that the kinetics of 5α-OOH decay did not deviate from apparent first order throughout the course of iron/AH$^-$ incubation (Figure 3). This, along with our inability to detect any radiolabeled 5α-OOH or 5α-OH when [^{14}C]Ch-LUVs were used, suggests that 5α-OOH could not have been regenerated to any significant extent during the reaction, e.g., via any $^1O_2$ arising from peroxyl radical disproportionation (*55*). On the basis of these considerations, we were able to exploit 5α-OOH decay rate as a sensitive indicator of whether •NO's antiperoxidative effects might simply be due to iron ligation. It was important to assess iron status in this study because chain initiation was iron-catalyzed. Inactivation of catalytic metal ions has not always been ruled out as an explanation for •NO's antiperoxidative effects, although this would clearly not be a concern when peroxyl radical-generating azo initiators are used (*14*). HPTLC-PI, which was introduced relatively recently (*20*), allowed us to measure several other ChOX in addition to 7αβ-OOH and thereby expand the information base on chain peroxidation in our system. HPLC-RC also permitted this, but with considerably lower sensitivity and resolving power than HPTLC-PI. In the prototype HPTLC-PI approach used here, [^{14}C]Ch serves as a natural membrane "sensor" for free radical activity taking place in its vicinity. Cholesterol well represents the plasma membrane in this respect because >90% of it is found in this compartment in most eukaryotic cells. As indicated, Ch gives rise to a reasonably small set of intermediates/products whose quality and quantity, as determined by this approach, provides valuable mechanistic information about the peroxidative process and how this might be altered by free radical interceptors such as •NO.

Although •NO derived from up to 100 μM SPNO had no effect on LUV 5α-OOH reduction by iron/AH$^-$, it slowed the production of both TBARS and certain ChOX compounds (5,6-epoxide and 7αβ-OOH), indicating that it could attenuate chain reactions involving both polyunsaturated phospholipids and Ch. •NO inhibition of TBA-detectable phospholipid peroxidation in micellar and liposomal systems has been described (*13*, *14*), but this appears to be the first evidence for Ch peroxidation being similarly affected. It has been reported (*56*) that •NO is capable of reducing EDTA-ligated Fe(III), thereby producing the strong oxidant hydroxyl radical (HO•) via the Fenton reaction, i.e., Fe(II) reduction of H_2O_2. We asked, therefore, whether similar chemistry might be possible in our system, and if so, how it might have affected the results. When 5α-OOH-laden LUVs were incubated with 1 μM Fe(HQ)$_3$ and 100 μM SPNO, but without AH$^-$ (cf. Figure 3), no net ChOX were detected after 30 min (not shown). Thus, the observed antioxidant effects of SPNO-derived •NO could not have been compromised by any prooxidant activity. As an antioxidant, such •NO appears to have acted mainly as a chain terminator by way of LO•/LOO• interception.

It might seem curious that •NO produced a sizable decrease in the rates of 5,6-epoxide, 7α-OOH, and 7β-OOH accumulation, yet had no effect on 7α-OH or 7β-OH (Figure 5). By contrast, BHT slowed the accumulation of all these species, which is perhaps not surprising, since they all derived from free radical reactions. In seeking an explanation for the noneffect of •NO on the 7-diols, one can gain insights from the reaction scheme shown in Figure 8. From the rate constants provided, one would expect 7-OO• to react much more rapidly with •NO than with LH ($k \sim 2 \times 10^9$ M^{-1} s^{-1} vs ∼50 M^{-1} s^{-1}). Similar considerations would apply for POPC peroxyl radicals generated in our system. Accordingly, •NO-induced decreases in the steady-state levels of 7-OO• and other LOO• would explain the observed declines in 5,6-epoxide and 7-OOH accumulation. Although 7-OOH levels were reduced by •NO (Figures 3 and 5), it is likely that they still remained much higher than the level of catalytic iron in the LUV membrane. Fe(HQ)$_3$ was added at a concentration of 1 μM, but it is not clear that all of this was redox-active in the reaction system. Also, competition of other peroxides (5α-OOH, POPC−OOH) for Fe(II) would have effectively reduced the amount of it available to 7-OOH. A reasonable deduction based on these considerations is that active iron remained "saturated" with 7-OOH even in the presence of •NO, such that the kinetics of 7-OH product formation were zero-order with respect to 7-OOH. This would explain the apparent inability of SPNO-derived •NO to slow 7α- or 7β-OH formation, at least over the first 45 min (Figure 4). However, continually declining 7-OOH level could account for the decrease in 7-OH level observed after much longer reaction periods (Figure 7). It is important to point out that the relatively slow release of •NO by SPNO ($t_{1/2} \sim 38$ min) should have allowed sufficient 7-OOH to accumulate in the early stages of the reaction so as to meet the zero-order conditions described. Accordingly, we found that the initial rate of 7-OOH buildup was not diminished by SPNO (Table 1). This may not have accrued if the same amount of •NO had entered the system in a relatively rapid burst, say from a fast-releasing donor (*5*, *10*, *11*). Under such conditions,

•NO would be expected to act more as a primary chain preventative by trapping 5α-O• or possibly Fe(II), thereby decreasing production of all ChOX species, including the 7-diols. Our results with SNAP (Table 1) could be explained along these lines. Interference with primary initiation, as predicted for a rapid •NO flux, probably accounts for the results obtained with BHT (Table 2). When used in a reaction, BHT, unlike slowly emitted •NO from SPNO, was present in relatively high concentration from the outset.

As indicated in Figure 8, 7-OO• scavenging by •NO would give rise to a highly reactive peroxynitrite intermediate (7-OONO). By analogy with similar compounds generated from N_2O_4 and simple organoperoxides (*45*), 7-OONO would undergo −O−O− bond homolysis, forming a caged radical pair [7-OO• •NO_2], which either recombines to give the 7-nitrate (7-ONO_2) or dissociates to free 7-O• and •NO_2. The 7-O• could either react with LH to initiate new chains or be scavenged by •NO. The rate constant of the latter reaction is ∼10^7-fold greater than that of the former (Figure 8). Using a conservative value of ∼1 μM for the steady-state concentration of •NO in our system when 100 μM SPNO was used, and knowing that the LH concentration was ∼2 mM, we estimate that •NO scavenging of 7-OONO-derived 7-O• would have been at least 3000 times faster than chain initiation. Such scavenging could be considered as a secondary (or backup) form of chain prevention. The •NO_2 produced by 7-OONO homolysis could conceivably act as an LH oxidant; however, no specific evidence for chain initiation by •NO_2 has appeared in the literature. A similar chain-terminating mechanism for •NO has been proposed for azo-initiated lipid peroxidation (*14*). From kinetic considerations, it was deduced in that study that at least two •NO molecules are consumed per molecule of LOO• destroyed, with concomitant formation of NO_2^-, $LONO_2$, and LONO. This stoichiometry clearly differs from that applying to phenolic antioxidants (α-tocopherol, BHT), each of which typically terminates two LOO• (*42*). It is important to note, furthermore, that a phenolic antioxidant inactivates LOO• by converting it to LOOH, which under iron-reducing conditions (as used in this study) may contribute to chain initiation. Thus, chain reactions are attenuated by phenolics but not necessarily abolished. Assuming that 7-OONO-derived •NO_2 is less reactive toward LH than LO• or LOO•, •NO would be a more effective antioxidant than, for example, BHT because LOOHs are not generated during •NO action, and nitrosated species such as 7-ONO or 7-ONO_2 (or reduction/hydrolysis products thereof) are not strong oxidants.

We routinely found that •NO inhibition of HPTLC-PI-detected chain peroxidation was accompanied by the appearance of a new, well-resolved Ch product referred to as RCh.4. Certain information about RCh.4, e.g., (i) direct formation via one-electron reduction of 7α-OOH (but not 7β-OOH) in the presence of •NO and (ii) quantitative conversion to 7α-OH by heating, e.g. 75 °C for 90 min on a TLC plate (results not shown), was consistent with it being a nitrosated derivative, specifically 7α-ONO. (Another possibility, 7α-ONO_2, was considered less likely because it could not have arisen via direct reduction of 7α-OOH.) However, a combination of HPLC-RC and HPTLC-PI analyses suggested that RCh.4 was not 7α-ONO, but rather the diol 5α-OH, and this was confirmed by means of EI-MS. 5α-OH is a well-known byproduct of $^1O_2$ attack (*22*). It can thermally isomerize to 7α-OH (*57*), and we have confirmed this, thereby accounting for observation (ii) above. There was no evidence for any significant $^1O_2$ production in our reaction systems, in either the absence or presence of •NO. No 5α-OOH or 5α-OH could be detected, for example, when 7α-OOH was used as a primer without •NO (results not shown). Therefore, how was 5α-OH generated in the presence of •NO, and does this have any bearing on the nitrosation reaction in question? One possible mechanism based on the premise that 7α-ONO was a prominent yet short-lived intermediate arising from 7α-OO•/7α-O• scavenging by •NO is shown in Figure 9. According to this scheme, 7α-ONO would have undergone not only reduction to 7α-OH with release of •NO (*34*, *58*) but also allylic rearrangement to the 5α isomer (5α-ONO), which in turn would have been converted to 5α-OH. The reductive conditions required for carrying out our reactions are assumed to have been incompatible with the accumulation of detectable amounts of either 7α-ONO or 5α-ONO. Reduction to 7α-OH may have predominated over the proposed rearrangement reaction (Figure 9), making 5α-OH a relatively minor product, as observed (<0.2% yield). We suggest that the appearance of 5α-OH in our system uniquely implicates 7α-ONO as a reactive intermediate. This appears to be the first reported evidence for redox generation of 5α-OH without $^1O_2$ intermediacy. Switching from reductant-based chain initiation (as used here) to oxidant-based initiation (*13*, *14*) might allow greater accumulation of nitrosated species such as 7α-ONO and 5α-ONO, thereby facilitating their detection. We are currently investigating this possibility.

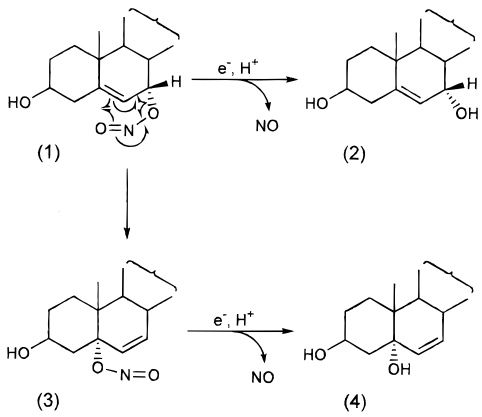

FIGURE 9: Proposed pathways for the conversion of 7α-ONO to 7α-OH and 5α-OH under the reaction conditions described. 7α-OH (2) would derive from the direct one-electron reduction of 7α-ONO (1) with release of •NO, whereas 5α-OH (4) would derive from allylic rearrangement of 7α-ONO to 5α-ONO (3) followed by one-electron reduction of the latter.

Our findings provide new mechanistic insights into how •NO might act as a cytoprotective antiperoxidant in biological systems. The strategies used allowed us to distinguish between effects such as chain termination via the interception of propagating radicals and chain prevention through iron chelation or interception of primary radicals. Chain-breaking activity has typically been invoked by others to explain •NO's antiperoxidative effects (*13*−*18*), but alternatives such as metal ion ligation/inactivation or scavenging of nonlipid initiating radicals have not always been ruled out. Further application of the approaches described in this study could lead to a better appreciation of how •NO might limit peroxidative damage associated with disease states such as atherosclerosis and cancer (*4*, *5*).

ACKNOWLEDGMENT

Helpful discussions with Neil Hogg throughout the course of this work are greatly appreciated. We also thank Frank Laib for carrying out the EI-MS analyses and for assisting us in interpreting the results.

REFERENCES

1. Mancada, S., Palmer, R. M. J., and Higgs, E. A. (1991) *Pharmacol. Rev. 43*, 109−142.
2. Lowenstein, C. J., and Snyder, S. H. (1992) *Cell 70*, 705−707.
3. Moilanen, E., and Vapaatalo, H. (1995) *Ann. Med. 27*, 359−367.
4. Hogg, N. (1955) in *Analysis of Free Radicals in Biological Systems* (Favier, A. E., Cadet, J., Kalyanaraman, B., Fontecave, M., and Pierre, J. L., Eds.), pp 37−49, Birkhauser-Verlag, Basel, Switzerland.
5. Wink, D. A., and Mitchell, J. B. (1998) *Free Radical Biol. Med. 25*, 434−456.
6. Huie, R. E., and Padmaja, S. (1993) *Free Radical Res. Commun. 18*, 195−199.
7. Koppenol, W. H., Moreno, J. J., Pryor, W. A., Ischiropoulos, H., and Beckman, J. S. (1992) *Chem. Res. Toxicol. 5*, 834−842.
8. Beckman, J. S., Ye, Y. Z., Anderson, P. G., Chen, J., Accavitti, M. A., Tarpey, M. M., and White, C. R. (1994) *Biol. Chem. Hoppe-Seyler 375*, 81−88.
9. Wink, D. A., Hanbauer, I., Krishna, M. C., DeGraff, W., Gamson, J. and Mitchell, J. B. (1993) *Proc. Natl. Acad. Sci. U.S.A. 90*, 9813−9817.
10. Wink, D. A., Cook, J. A., Krishna, M. C., Hanbauer, I., DeGraff, W., Gamson, J. and Mitchell, J. B. (1995) *Arch. Biochem. Biophys. 319*, 402−407.
11. Wink, D. A., Cook, J. A., Pacelli, R., Degraff, W., Gamson, J., Liebman, J., Krishna, M., and Mitchell, J. B. (1996) *Arch. Biochem. Biophys. 331*, 241−248.
12. Chang, J., Rao, N. V., Markewitz, B. A., Hoidal, J. R., and Michael, J. R. (1996) *Am. J. Physiol. 270*, L931−L940.
13. Rubbo, H., Radi, R., Trujillo, M., Kalyanaraman, B., Barnes, S., and Freeman, B. A. (1994) *J. Biol. Chem. 269*, 26066−26075.
14. O'Donnell, V. B., Chumley, P. H., Hogg, N., Bloodsworth, A., Darley-Usmar, V. M., and Freeman, B. A. (1997) *Biochemistry 36*, 15216−15223.
15. Rubbo, H., Parthasarathy, S., Barnes, S., Kirk, M., Kalyanaraman, B., and Freeman, B. A. (1995) *Arch. Biochem. Biophys. 324*, 15−25.
16. Hayashi, K., Noguchi, N., and Niki, E. (1995) *FEBS Lett. 370*, 37−40.
17. Kalyanaraman, B., Joseph, J., Struck, A., and Parthasarathy, S. (1993) *FEBS Lett. 334*, 170−174.
18. Hogg, N., Struck, A., Goss, S. P., Santanam, N., Joseph, J., Parthasarathy, S., and Kalyanaraman, B. (1995) *J. Lipid Res. 36*, 1756−1762.
19. Padmaja, S., and Huie, R. E. (1993) *Biochem. Biophys. Res. Commun. 195*, 539−544.
20. Korytowski, W., Wrona, M., and Girotti, A. W. (1999) *Anal. Biochem. 270*, 123−132.
21. Schenck, G. O., Gollnick, K., and Neumuller, O. A. (1957) *Justus Liebigs Ann. Chem. 603*, 46−59.
22. Kulig, M. J., and Smith, L. L. (1973) *J. Org. Chem. 38*, 3639−3642.
23. Korytowski, W., Bachowski, G. J., and Girotti, A. W. (1991) *Anal. Biochem. 197*, 149−156.
24. Girotti, A. W., Thomas, J. P., and Jordan, J. E. (1985) *Arch. Biochem. Biophys. 236*, 238−251.
25. Bachowski, G. J., Pintar, T. J., and Girotti, A. W. (1991) *Photochem. Photobiol. 53*, 481−491.
26. Korytowski, W., Geiger, P. G., and Girotti, A. W. (1999) *Methods Enzymol. 300*, 23−33.
27. Maragos, C. M., Morley, D., Wink, D. A., Dunams, T. M., Saavedra, J. E., Hoffman, A., Bove, A. A., Isaac, L., Hrabie, J. A., and Keefer, L. K. (1991) *J. Med. Chem. 34*, 3242−3247.
28. Mayer, L. D., Hope, M. J., and Cullis, P. R. (1986) *Biochim. Biophys. Acta 858*, 162−168.
29. Buettner, G. R. (1988) *J. Biochem. Biophys. Methods 16*, 27−40.
30. Lange, Y., Swaisgood, M. H., Ramos, B. V., and Steck, T. L. (1989) *J. Biol. Chem. 264*, 3786−3793.
31. Lin, F., and Girotti, A. W. (1993) *Arch. Biochem. Biophys. 300*, 714−723.
32. Halliwell, B., and Gutteridge, J. M. C. (1990) *Methods Enzymol. 186*, 1−85.
33. Geiger, P. G., Korytowski, W., and Girotti, A. W. (1995) *Photochem. Photobiol. 62*, 580−587.
34. Feelisch, M., and Stamler, J. S. (1996) in *Methods in Nitric Oxide Research* (Feelisch, M., and Stamler, J. S., Eds.) pp 71−115, Wiley, New York.
35. Johnson, R. F., Pickett, S. C., and Barker, D. L. (1990) *Electrophoresis 11*, 355−360.
36. Korytowski, W., Bachowski, G. J., and Girotti, A. W. (1993) *Anal. Biochem. 213*, 111−119.
37. Korytowski, W., Geiger, P. G., and Girotti, A. W. (1995) *J. Chromatogr. B 670*, 189−197.
38. Smith, L. L., Teng, J. I., Kulig, M. J., and Hill, F. L. (1973) *J. Org. Chem. 38*, 1763−1765.
39. Girotti, A. W. (1992) *J. Photochem. Photobiol. B: Biol. 13*, 105−118.
40. Traylor, T. G., and Sharma, V. S. (1992) *Biochemistry 31*, 2847−2849.
41. Teng, J. I., Kulig, M. J., and Smith, L. L. (1973) *J. Chromatogr. 75*, 108−113.
42. Burton, G. W., Doba, T., Gabe, E. J., Hughes, L., Lee, F. L., Prasad, L., and Ingold, K. U. (1985) *J. Am. Chem. Soc. 107*, 7053−7065.
43. Niki, E. (1987) *Chem. Phys. Lipids 44*, 227−253.
44. Frost, M. J., and Smith, I. W. N. (1990) *J. Chem. Soc., Faraday Trans. 86*, 1757−1762.
45. Pryor, W. A., Castle, L., and Church, D. F. (1985) *J. Am. Chem. Soc. 107*, 211−217.
46. Yamazaki, S., Ozawa, N., Hiratsuka, A., and Watnabe, T. (1999) *Free Radical Biol. Med 27*, 301−308.
47. Vile, G. F., and Tyrrell, R. M. (1995) *Free Radical Biol. Med. 18*, 721−730.
48. Pourzand, C., Watkin, R. D., Brown, J. E., and Tyrrell, R. M. (1999) *Proc. Natl. Acad. Sci. U.S.A. 96*, 6751−6756.
49. Garnier-Suillerot, A., Tosi, L., and Paniago, E. (1984) *Biochim. Biophys. Acta 794*, 307−312.
50. Forni, L. G. (1990) in *Membrane Lipid Oxidation* (Bigo-Pelfrey, C., Ed.) Vol. I, pp 15−32, CRC Press, Boca Raton, FL.
51. Hasegawa, K., and Patterson, L. K. (1978) *Photochem. Photobiol. 28*, 817−823.
52. Babbs, C. F., and Steiner, M. G. (1990) *Free Radical Biol. Med. 8*, 471−485.
53. Wilcox, A. L., and Marnett, L. J. (1993) *Chem. Res. Toxicol. 6*, 413−416.
54. Gardner, H. W. (1989) *Free Radical Biol. Med. 7*, 65−86.
55. Howard, J. A., and Ingold, K. U. (1968) *J. Am. Chem. Soc. 90*, 1056−1058.
56. Miles, A. M., Bohle, D. S., Glassbrenner, P. A., Hansert, B., Wink, D. A., and Grisham, M. B. (1996) *J. Biol. Chem. 271*, 40−47.
57. Smith, L. L., Kulig, M. J., and Teng, J. I. (1973) *Steroids 22*, 627−635.
58. Keefer, L. K., and Williams, D. L. H. (1996) in *Methods in Nitric Oxide Research* (Feelisch, M., and Stamler, J. S., Eds.) pp 509−519, Wiley, New York.

BI000393E